Numerical Simulation of Liquid Fueled SCRAMJET Combustor Flow Fields

Debasis Chakraborty*
Directorate of Computational Dynamics, Defence Research and Development Laboratory,
Hyderabad – 500058, INDIA.

Abstract
Numerical simulations were carried out for various reacting flow fields related to scramjet propulsion system using commercial CFD Software. Three-dimensional Navier stokes equations were solved along with the K-ε turbulence model. Modeling of the turbulence chemistry interaction is done through infinitely fast rate chemical kinetics. The software was validated extensively by comparing different experimental conditions for scramjet combustor to find its error band and range of application. Good agreement between the experimental and computational values were obtained for the scramjet combustor flow field with strut, pylon and cavity injection system with both hydrogen and hydrocarbon fuel. The validated CFD tool was applied in the design exercise of flight-sized kerosene fuel scramjet combustor of a hypersonic airbreathing mission. Significant improvement of combustion efficiency and thrust could be achieved by relocating the fuel injection system through the analysis of various thermochemical variables in the scramjet combustor.

1. INTRODUCTION

The success of an efficient design of a hypersonic airbreathing cruise vehicle largely depends on the proper choice of propulsion system. This type of vehicle, according to current proposals, will use scramjet propulsion system. Both hydrogen and hydrocarbon fuels are considered depending on applications and speed range. Although, hydrogen has attractive features in terms of specific impulse, ignition characteristics, etc., liquid hydrocarbon fuel is preferred for volume limited applications in the lower hypersonic region (M<8). Starting from the pioneering work of Ferri [1], significant advances are made in the design of scramjet engines. Over the last few decades, great emphases were placed on analytical, experimental and CFD techniques to understand the mixing and combustion processes in the scramjet combustors. In a recent review, Curran [2] has identified two emerging scramjet applications, namely (1) hydrogen fueled engine to access space and (2) hydrocarbon-fueled engines for air-launched missiles.

Considerable efforts have been focused on different injection schemes like cavity, strut and pylon for different geometrical configurations and flow conditions. Selected methods that have been used to enhance the mixing process in scramjet engines are summarized and reported in Ref 3. Results indicated that atomization, vaporization, mixing and slow chemical reactions are some of the major barriers in the realization of liquid hydrocarbon fuel based scramjets. The problem of slow lateral fuel transport in the air stream can be circumvented by injecting the fuel in the core region of the flow by means of struts and or pylons. The oblique shocks generated from the struts also augment the mixing process which is very much needed in high speed propulsion devices. A good number of experimental and numerical studies [4–11] are reported in the literature to focus on various aspects of flow phenomena including drag losses, mixing, combustion, intake combustor interaction etc., in strut based scramjet combustors with hydrogen fuel. The reported experimental and numerical studies on kerosene fueled supersonic combustion mostly address the issues of cavity based flame holder and injection systems [12–18] in laboratory scaled combustor.

*Corresponding Author: Debasis Chakraborty, Directorate of Computational Dynamics, Defence Research and Development Laboratory, Hyderabad - 500058, INDIA. Tel. +91-40-24583310, Fax. +91-40-24340037, E-mail. debasis_cfd@drdl.drdo.in

Studies on strut-based scramjet combustor with kerosene fuel are highly limited. Vinogradov *et al*. [19] conducts experimental investigation to determine the ignition, piloting, and flame holding characteristics in a strut based scramjet combustor operating on kerosene. In order to improve the fuel distribution and mixing, kerosene was injected from the strut located in the middle of the duct. Stable combustion of kerosene was achieved even after turning off the pilot hydrogen fuel. Bouchez, Dufour and Montazeal [20] carried out an experimental investigation of hydrocarbon fueled scramjet combustor. Two identical metallic water-cooled and liquid kerosene cooled struts were used for the fuel injection in the combustor. Pilot flames with gaseous hydrogen were used at the base of the struts to ensure ignition. Kerosene equivalence ratio was varied from 0 to 1.0. Various flow parameters such as wall pressure, wall heat flux, total temperature at combustor exit, thrust were measured. Optical methods including passive spectroscopy were also used to characterize the flow.

With the advent of powerful computers and robust numerical algorithms, CFD is complementing 'difficult to perform' experiment and thus playing a major role in developing a comprehensive understanding of the key phenomenon that dominate performances. Only very few numerical studies are reported on strut based liquid fueled scramjet combustor. Dufour and Bounchez [21] have numerically simulated the scramjet experiment [20] using a three dimensional Navier Stokes solver and single step chemical kinetics. A reasonably good match is obtained between the computational and experimentally measured wall static pressure. Recently, Manna, Behera and Chakraborty [22] presented a CFD based design and analysis for a flight scale scramjet combustor with kerosene fuel injected from struts placed in the combustor flow path. Their results emphasized that higher combustor entry Mach number and distributed fuel injection system is required to avoid thermal chocking.

But before the CFD software is used in the design exercise, it is necessary to make thorough validation checks to find its range of application and error band. This paper present the validation studies for a few hydrogen and kerosene fuelled scramjet combustor and the use of CFD techniques for the development of a full scale scramjet combustor for a hypersonic airbreathing mission.

2. METHODOLOGY

The software, used in the present study, is a three dimensional Navier Stokes code – CFX-TASC flow [23] which is an integrated software system capable of solving diverse and complex multidimensional fluid flow problems. The code is fully implicit, finite volume method with finite element based discretisation of geometry. The method retains much of the geometric flexibility of finite element methods as well as the important conservation properties of the finite volume method. It utilizes numerical upwind schemes to ensure global conservation of mass, momentum, energy and species continuity. It also implements a general non-orthogonal, structured, boundary fitted grids. In the present study, to circumvent the initial numerical transient, the descretisation of the convective terms are initially done by first order upwind difference scheme and subsequently, the convective terms are discretized through 2nd order scheme to capture the flow features more accurately. The K-ε turbulence model with wall functions is used in the simulation.

The chemistry of the hydrogen-air combustion reaction is represented on a molar basis by $H_2 + 0.5O_2 = H_2O$; whereas kerosene–air combustion reaction is represented by: $C_{12}H_{23} + 17.75O_2 = 12CO_2 + 11.5H_2O$. The mixing rate determined from the Eddy Dissipation Model (EDM) is given as.

$$R_{k,edm} = -A_{ebu}\rho\frac{\varepsilon}{K}\min\left\{Y_f, \frac{Y_o}{r_k}, B_{ebu}\frac{Y_p}{1+r_k}\right\}$$

where ρ, Y_f, Y_o and Y_p are the density and mass fractions of fuel, oxidizer and products respectively, A_{ebu} and B_{ebu} are the model constants and r_k is the stoichiometric ratio.

The Lagrangian tracking method is used for the discrete phase model to characterize the flow behaviour of the dispersed phase fluid (kerosene liquid). The prediction of flows involving the dispersed phase includes separate calculation of each phase with source terms generated to account for the interaction between the phases. The flow of the continuous phase is predicted using a discretized

form of the Navier Stokes equations. However, with the dispersed phase there is no continuum, and each particle interacts with the fluid and other particles discretely. The behaviour of the dispersed phase is determined by tracking several individual particles through the flow field. Each particle represents a sample of particles that follow an identical path. The behaviour of the tracked particles is used to describe the average behaviour of the dispersed phase. Both pressure drag and viscous drag on the particles are considered while particle-to-particle interactions and effect of turbulence in the discrete phase are not simulated in the analysis.

3. RESULTS AND DISCUSSIONS

3.1. Validation Studies

Four different experimental conditions are selected for comparisons with numerical simulations so that most of the issues related to Scramjet propulsion could be addressed.

- Staged supersonic combustor with hydrogen fuel from strut and wall injectors [24]
- Hydrogen fuelled Scramjet combustor with pylon injector [25]
- Kerosene fuelled scramjet combustor with cavity injector [26]
- Kerosene fueled scramjet combustor with ramp-cavity combustor [27]

3.1.1. Staged Supersonic Combustor with Strut Injection

Strut based Scramjet combustors with hydrogen fuel [4-8] were extensively investigated experimentally at NAL, Japan focusing on various aspects of drag losses, mixing, combustion, and intake-combustor interactions among others. Injection of excessive fuel form the strut can cause inlet-combustion interaction that may lead to engine unstart condition. To reduce such intake-combustor interaction, a staged supersonic combustor with strut for the first stage injection and wall at divergent section for second stage injection was experimentally studied by Tomioka et al. [8, 9] in a direct-connect wind tunnel facility. The combustor tests were carried out for a combustor entry Mach number of 2.5, total temperature of 1500 K and total pressure of 1.0 MPa which are similar to the combustor entrance condition under Mach 6 flight condition at an altitude of about 30 Km. Hydrogen was injected at sonic condition from the strut and the wall with various equivalence ratios from 0.35 to 1.25. The schematic diagram of the combustor for which the computations were carried out is shown in Fig. 1. A strut with a blunt leading edge (1 mm in radius) and a compression part (43.8 mm) with half wedge angle of 6°, followed by a 28 mm straight portion is installed in the constant area section. Downstream of the contrast area section, the sidewall diverged at an angle of 3.1° for 600 mm. Various test cases

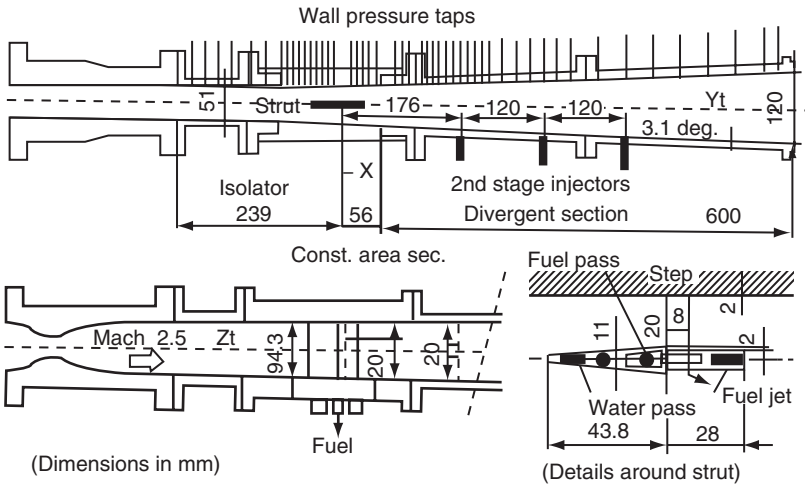

Figure 1. Schematic of the scramjet combustor with the strut.

Table 1. Test conditions for staged supersonic combustor

Cases	First stage injection	Second stage injection
Non reacting	None	None
Reacting	Strut injection (φ = 0.35)	None
Reacting	Strut injection (φ = 0.35)	Wall injection at x = 296 mm (φ = 0.44)
Reacting	Strut injection (φ = 0.35)	Wall injection at x = 416 mm (φ = 0.9)

with different fuel injection options in the strut and divergent portion of the combustor wall are shown in Table 1. Taking advantage of two planes of symmetry, only one fourth of the geometry is simulated [24]. The computed axial pressure distribution for the non-reacting case is compared with the experimental values in Fig. 2. Pressures have been nondimensionalized by total pressure and the origin (X = 0) is taken at the location of step. It can be seen that by changing the grids from 1,71,105 to 2,95,071, results have not changed appreciably near the fuel injection region of the combustor. There is an upstream shift of 50 mm of the location of the terminal shock for fine grid near the combustor exit. Since the purpose of the study is to capture the reacting flow field in the fuel injection region, no grid refinement studies were undertaken to resolve the difference and the finer grid was used for the remainder of the computation. A very good agreement between the experiment and the computation has been obtained. All the shock interaction in the combustor has been captured very nicely in the computations.

Reacting flow computations are carried out with various fuel injections from the strut and the wall. The temperature and water mass fraction distribution in the combustor for the strut injection case are shown in Fig. 3. It is clear from the figure that the reaction occurs only in the central zone of the combustor. The flow field in the rest of the combustor almost remains unreacted. The surface pressure comparison between the experiment and the computation is presented in Fig. 4. A very good match is observed except near the fuel injection location, where the computation overpredicts the surface pressure. This difference is due to the use of fast chemistry, which cause instantaneous heat release in the modeling resulting in prediction of higher surface pressure. Kumaran and Babu [28]

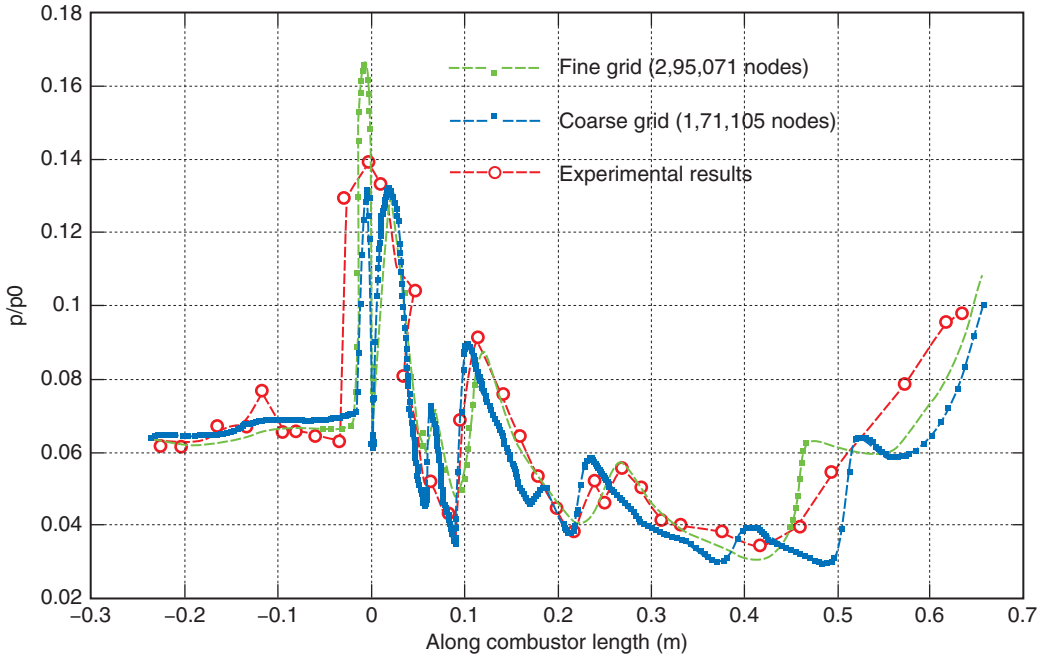

Figure 2. Comparison of wall pressure distributions for the non reacting case.

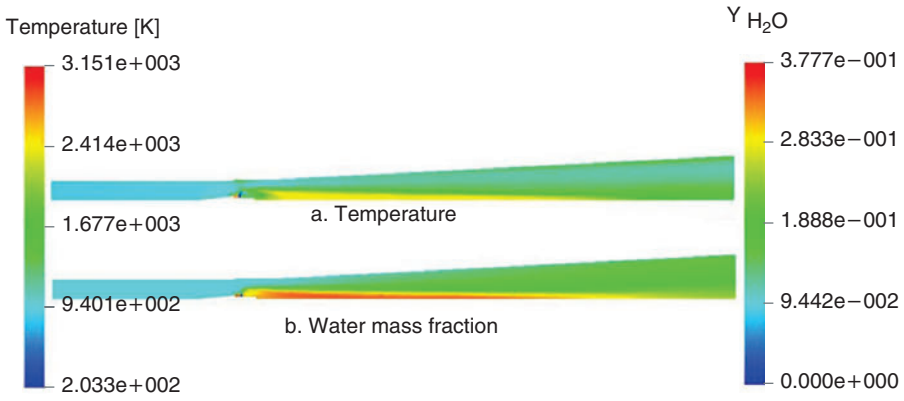

Figure 3. Flow variables in the symmetry plane for the reacting case with strut injection (φ_1 = 0. 34) (a) Temperature (b) Water mass fraction.

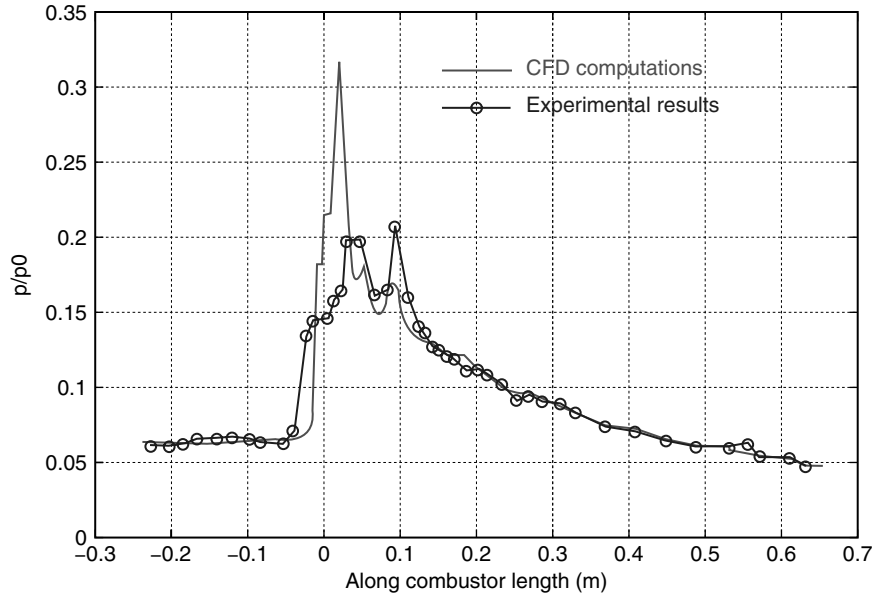

Figure 4. Wall pressure comparison for the reacting case (fuel injection from strut (φ_1 = 0. 34)).

studied the effect of multi step and single step H_2 – Air chemistry without turbulence chemistry interaction. The predicted pressure rise in the injection zone is higher with single step chemistry compared to multi step chemistry.

The surface pressures for various reacting and non-reacting cases are compared in Fig. 5. With the second stage injection from the wall, there is considerable increase in pressure in the divergent section, which is very necessary to increase the thrust. For the case of injection from both the strut and the wall (Φ_1 = 0.35 + Φ_2 = 0.44), wall pressure is seen to increase at x = 200 mm, while for the higher equivalence ratio (Φ_1 = 0.35 + Φ_2 = 0.90), the point of increase of wall pressure is seen to move upstream but did not effect the pressure peak caused due to strut injection. Effort to inject more fuel from the strut resulted in the upstream movement of the combustor shock in the intake and could cause intake unstarting. The staged injection is controlling the pressure rise in the wall and preventing intake – combustor interaction.

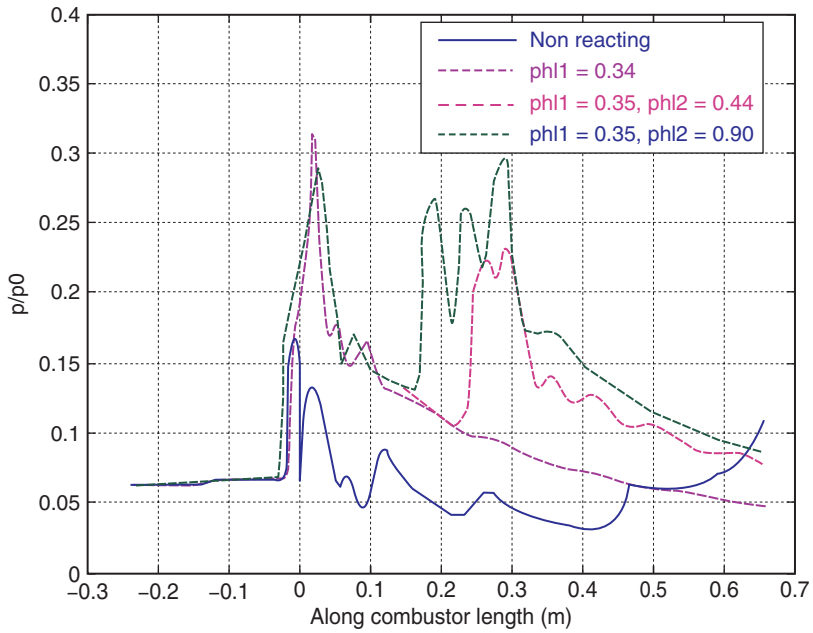

Figure 5. Comparison of wall pressure distribution for all reacting and non reacting cases.

3.1.2. Supersonic Combustion with Pylon Injection

Selecting proper injector geometry is one of the most important considerations for scramjet engine development. Fuel injection from the wall will result in reaction zones that occupy only a small fraction of the flow field. Therefore, not all of the oxygen supplied by the air stream entering the combustor can participate in the chemical reaction. The problem of slow lateral fuel transport in the airstream can be circumvented by injecting the fuel in the center of the flow by mean of pylons. Although, a few pylon designs have been investigated experimentally [29, 30] to study their effectiveness in fuel mixing and combustion in scramjet combustors, numerical simulations of the reacting flow fields for pylon injected scramjet combustors are very limited. Numerical simulations of the experimental condition of Grunneig et al. [29] were carried out by Javed and Chakraborty [25]. The combustor is 645 mm long, 25 mm width and its height is 27.5 mm at the entry and 40.5 mm at the exit. The pylon is placed at a distance of 45 mm from the combustor entry. An expansion angle of 5° is provided on the lower surface of the combustor for 150 mm just after the pylon. The combustor and the grid distribution with a more detailed view near the pylon, is shown in Fig. 6. Sonic hydrogen, with a 3.9 bar total pressure and 288 K total temperature is injected at 120° from slot shaped orifice into a vitiated air of Mach no, total pressure and total temperature of 2.15, 7.8 bar and 1350 K respectively. The Water mass fraction

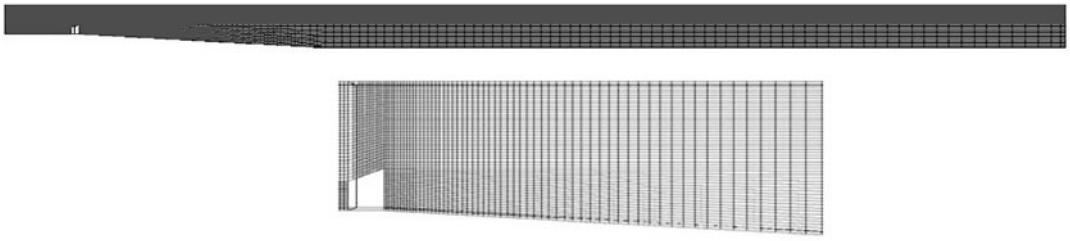

Figure 6. Grid distributions in the injection plane with detailed view near pylon.

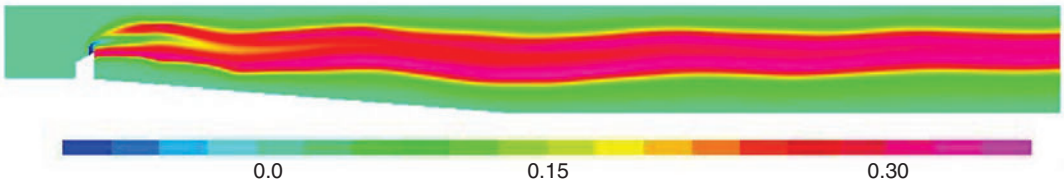

Figure 7. Water mass fraction distributions in the injection plane.

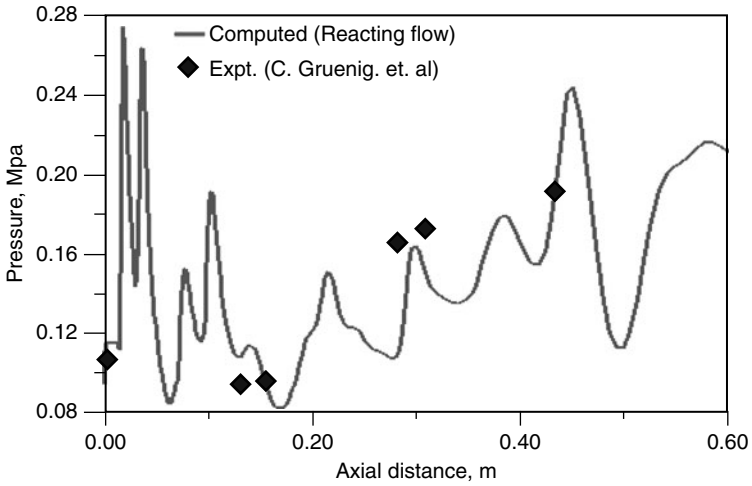

Figure 8. Comparison of axial distribution of surface pressures for the pylon based scramjet combustor.

distribution in the plane of injection is presented in Fig. 7, which clearly depicts the reaction zone occupying a significant portion of the combustor flow field. A comparison between the experimental and computational values of surface pressure at the top wall is shown in Fig. 8. A reasonable match is obtained.

3.1.3. Kerosene Fuelled Scramjet Combustor with Cavity Injector

A schematic of cavity based scramjet combustor experiment [13], for which the computations were carried out is shown in Fig. 9. The combustor has a rectangular cross section with an entry cross section of 51 × 70 mm^2. The length of the combustor is 1070 mm and consists of four sections. Different types of integrated wall injector cavity configuration were designed and tested at various stagnation conditions with liquid kerosene fuel. Numerical investigations [26] were carried out with three different cavity configurations (cavity modules A, B and C). The depth of the cavities is 12 mm and the lengths of the cavities are 88, 61 and 95 mm giving the L/h ratios of 7.33, 5.08 and 7.92 respectively. Kerosene was injected normally to the vitiated air stream via five orifices of 0.6 mm diameter. For cavity module-A, fuel was injected upstream of cavity at an equivalence ration of 0.45, while for the cavity-B and cavity-C, the fuel injected at the base of the cavity at equivalence ratio of 0.45 and 0.78 respectively. The total temperature, total pressure and Mach number of the vitiated air were 1840 K, 10.44 bar and 2.5 respectively. More detailed descriptions of the experiments are available in Ref. [13].

Cross sectional views of the mass fractions of CO_2 (the reaction product) are presented in Fig. 10 to depict the zone covered by reaction. Although, the kerosene is injected at 49 mm upstream of the cavity, the presence of CO_2 is seen 136 mm upstream of the injection point as the fuel has diffused through the recirculation separation bubble. Although, there is some CO_2 across the complete width of the

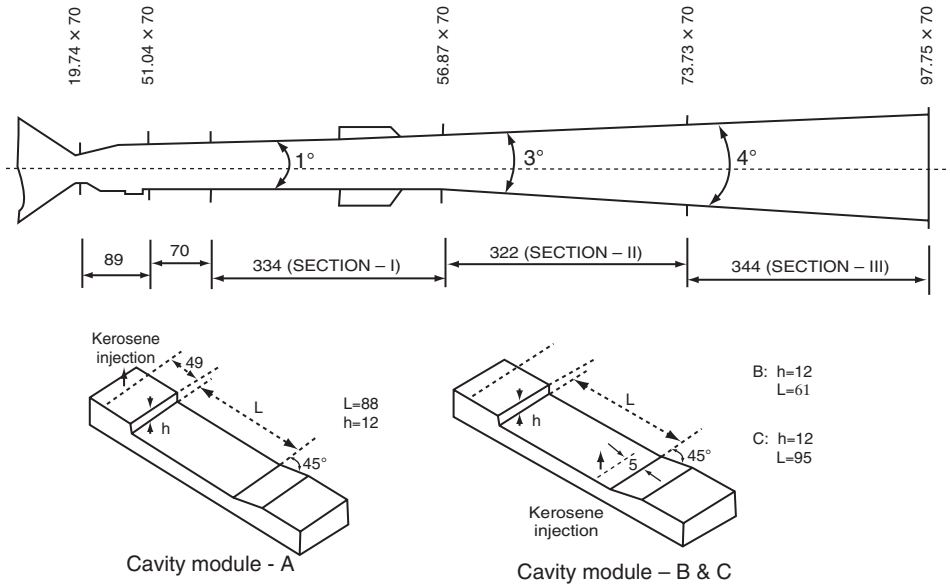

Figure 9. The cavity based scramjet combustor [13] for which computations are carried out.

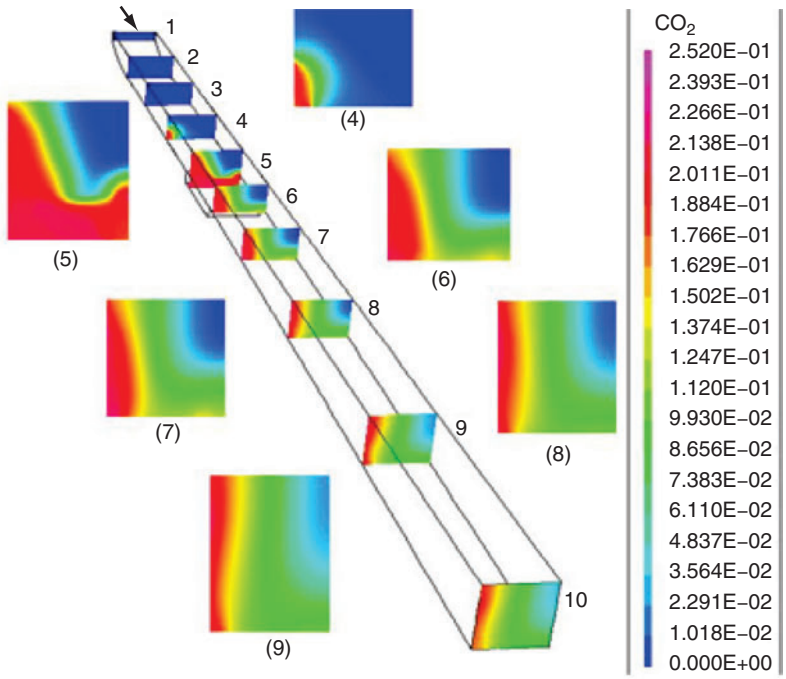

Figure 10. CO_2 mass fractions at various axial stations from facility nozzle throat to exit.

combustor, reaction is not very intense. This is mainly because of the relatively low equivalence ratio of 0.45. The computed side wall surface pressure for cavity-A, cavity-B and cavity-C configurations are shown in Fig. 11 (a) to 11 (c). As mentioned earlier, the equivalence ratios for the cavity A and cavity B configurations are 0.45, whereas the equivalence ratio for cavity C is 0.78. The surface

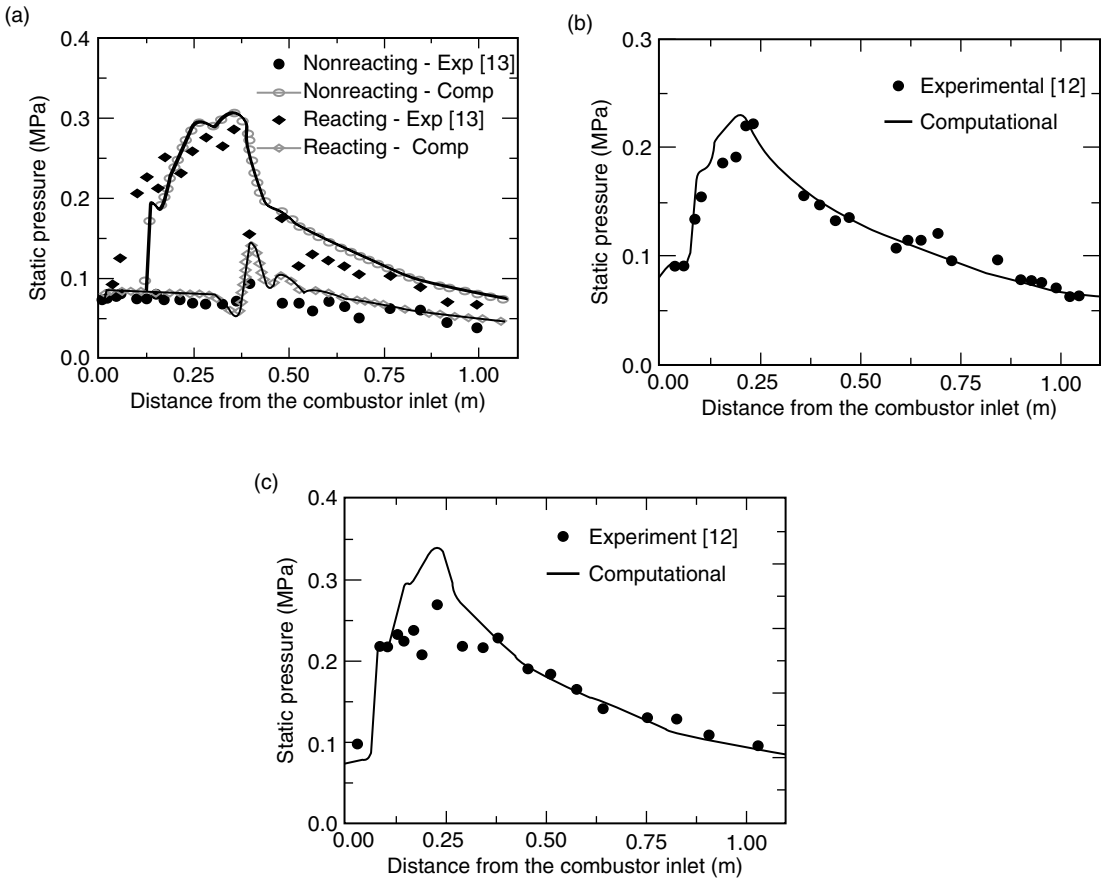

Figure 11. Surface pressures Comparison (a) Cavity-A (b) Cavity-B (c) Cavity-C.

pressure for the non-reacting case for the cavity A configuration is also shown in Fig. 11 (a). The increase in static pressure starts 200 mm upstream of injection location showing significant upstream interaction due to heat release. The static pressure reaches an approximately isobaric plateau in the nearly constant area section near X = 250 mm and decrease continuously until the combustor exit because of flow expansion in the divergent section of the combustor. Good comparisons between experimental and computational values are obtained except in the region of fuel injection where the computational values are 10–15% higher. The higher heat release caused due to fast chemistry assumption in the simulation is conjectured to be the cause of higher surface pressure in the injection zone. In the divergent portion, the principle thrust producing element of the combustor, the agreement between the two is very good. The difference between the surface pressures for the non-reacting and reacting cases presented for the cavity module-A in Fig. 11(a) quantifies the effect of heat release on the surface pressures in the combustor. The effect of droplet diameter on the surface pressure was determined by carrying out the simulation with different particle diameters of 1, 5, 10 and 20 μm for the cavity module-A configuration with equivalence ratio 0.45. The computed surface pressures with different droplet diameters are compared with experimental values in Fig. 12. It can be observed that with smaller droplet diameter, the evaporation is faster and the heat release is intensive. This has lead to more surface pressure rise near the injection zone. The higher heat release is also responsible for more upstream interaction for the smaller droplet diameter case. The effect of the droplet diameter on the surface pressure is insignificant in the divergent portion of the combustor.

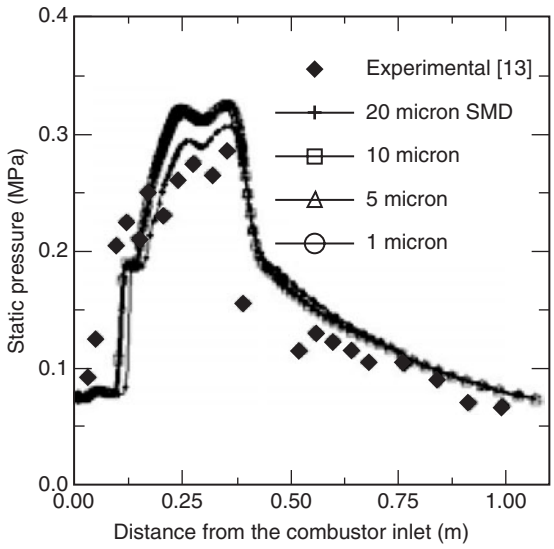

Figure 12. Effect of droplet diameter on the surface pressure for cavity-A.

3.1.4. Ramp-Cavity Scramjet Combustor with Kerosene Fuel

The combustor configurations for which the computations [27] were carried out are taken from Ref. 31. The combustor configuration is presented in Fig 13. The combustor consists of three parts namely, the facility nozzle, the constant area section and the divergent section with divergence angle of 3.2°. Three and two distributed ramps were provided on the bottom and top walls respectively in the constant area portion of the combustor as shown in Figs 13(b) and (c). One cavity each of length to depth ratio of 7.25 is located in both the top and bottom walls at the end of the ramps for flame holding purpose. Kerosene is injected in the combustor through 10 injectors of 0.4mm diameter. The vitiated air from the burner accelerated through a Mach 2.0 two dimensional convergent-divergent nozzle into the combustion chamber. The total temperature and total pressure of the vitiated air is 0.9 MPa and 1645 K respectively. The equivalence ratio is 0.21.

Mach number distributions for the reacting and non-reacting cases in the plane of symmetry are compared in Fig 14. The flow structure is different between the two cases. The terminal shock for the

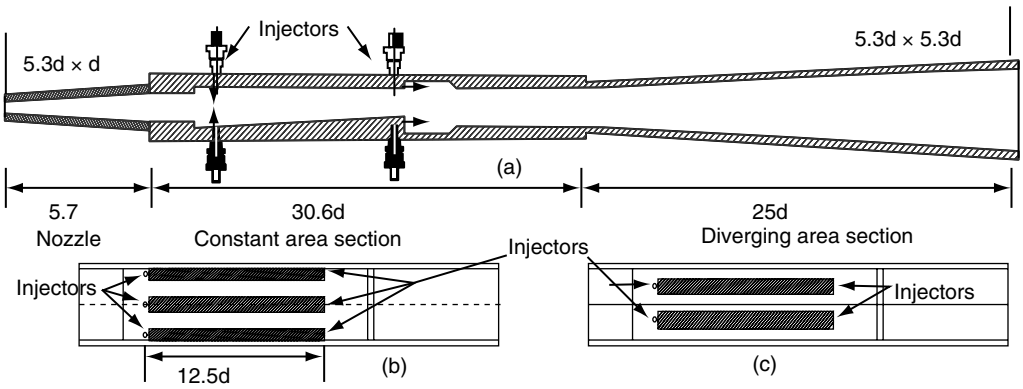

Figure 13. Ramp cavity scramjet combustor configuration: (a) Full combustor, (b) Bottom plate of constant area section, and (c) Top plate of constant area section.

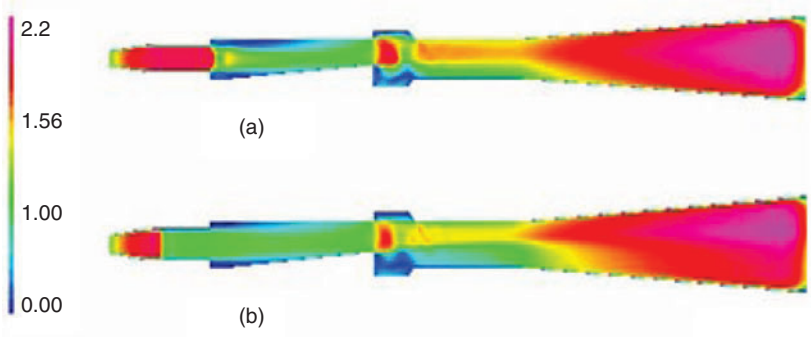

Figure 14. Mach number distribution in the symmetry plane: (a) non-reacting and (b) reacting.

reacting case is in upstream location of that for the nonreacting case because of heat release due to reaction. The flow accelerates again in the divergent section of the combustor. The axial distribution of the computed non-dimensional pressure at the top surface of the plane of symmetry is compared with the experimental values in Fig 15. The axial length has been normalized with the height of the throat of the facility nozzle and the surface pressure is nondimensionalised with total pressure p_0. A very good match has been obtained between experimental and numerical values except near the injection location, where the computation predicts higher value because of fast chemistry assumption.

3.2. Application of CFD Technique for Flight Sized Scramjet Combustor Design

The validation exercises in the previous section demonstrate that although predicted pressure rise is more in the fuel injection zone because of the fast chemistry assumption, the computed pressures match reasonably well in the divergent portion of the combustor where the major portion of thrust is produced.

The numerical methodology was used to design a flight sized scramjet combustor for an engine-integrated hypersonic cruise airbreathing mission explained in Ref 32. Autonomous functioning of a kerosene fuelled scramjet engine is envisaged for 20 sec in Mach 6.5 free stream condition at an altitude of 32,5 Km. Considering the limitation of the connected pipe mode facility, the development of the scramjet combustor is focused on the half module. A typical geometry of the combustor is shown in Fig 16. Kerosene fuel is injected from a V shaped strut with obtuse total angle. Marquardth Corporation, USA used this type of strut to increase the three dimensionality of the flow field [33]. The combustor entry conditions are obtained from a numerical simulation of the forebody and air intake

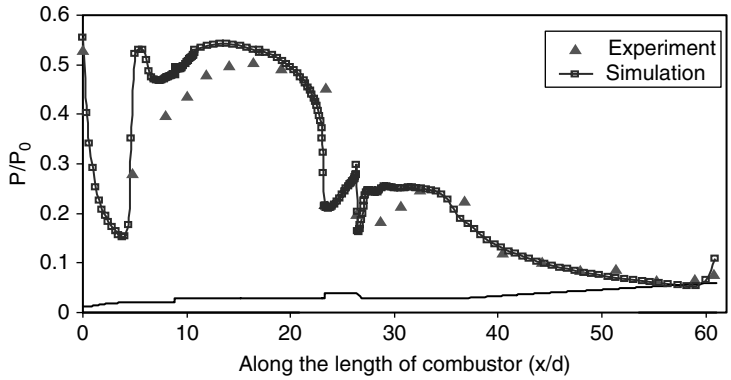

Figure 15. Comparison of surface pressure distributions in the symmetry plane for the reacting case.

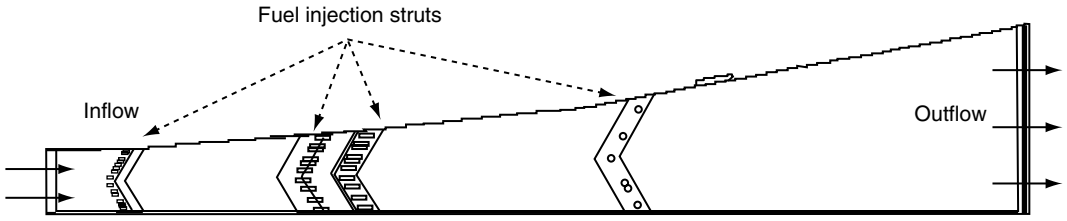

Figure 16. Typical geometry of the scramjet combustor.

flow field of the cruise vehicle and are presented in Table 2. The combustor entry Mach number is 2.0; while the total pressure and total temperature and fuel equivalence ratio are 0.38 MPa and 1940 K and 1.0 respectively. Kerosene fuel at room temperature is injected in the combustor through more than 100 injection points in the struts placed at various locations in the combustor flow path.

Taking the advantage of the symmetry of geometry, only one half of the combustor is simulated. A multiblock structured gird is employed in the simulation. The grid is very fine near the wall and near the leading and trailing edges of the strut and relatively coarser grids are provided in the remaining portion of the combustor. Since the injection holes are very small in diameter, original grids are made finer by doing the grid embedment adjacent to each injection point. The grid embedment has approximated the circular hole as the rectangular hole with the same equivalent area. Because the area of the hole is very small, this approximation is not likely to effect the flow development. In the simulation, X axis is taken along the length of the combustor while the Y and Z axes are chosen along the width and height of the combustor respectively. The origin is placed at the inlet of the combustor at the middle of the bottom surface. The grid is found to be adequate to resolve all the features of the flow field as found from the grid independence (not shown in the paper) of the simulation.

A number of reacting and nonreacting simulations were carried out to understand the complex mixing and combustion process inside the combustor. Flow is assumed to be uniform at the combustor entry and the ignition of kerosene is assumed. Typical Mach number distributions for the reacting flow in the symmetry plane and at different axial locations (X/h=0.0, 3.5, 5.8, 8.1, 10.5, 12.8, 16.3 and 21.5) are shown in Fig 17. It can be seen that although the Mach number reduces in the reaction zone due to reaction and heat release, the flow does not choke and general supersonic flow prevails in the combustor. The axial distributions of surface pressures at the top wall, bottom wall and side wall, along with the mass averaged cross sectional pressure values are shown in Fig 18. Significant variations of surface pressures in different walls indicate three dimensionality of the flow in the combustor. It has been observed from various flow parameters that reactions have occurred mostly in the central portion of the combustor. In the near wall region although oxygen is available, reactions did not take place due to lack of fuel penetration into the region. The computed combustion efficiency is only 51.43% and the achieved thrust is inadequate for the proposed mission.

Based on these observations, the struts were relocated by increasing the distance in the width direction and the struts near the side wall were placed so that the near wall region would get adequate kerosene fuel for reaction. Cross sectional views of CO_2 mass fractions at various axial locations are

Table 2. Inflow parameter at combustor entry

Parameter	Value
Mach No.	2.0
Total Temperature (K)	1940
Total Pressure (Mpa)	0.38
Fuel Equivalence Ratio	1.0

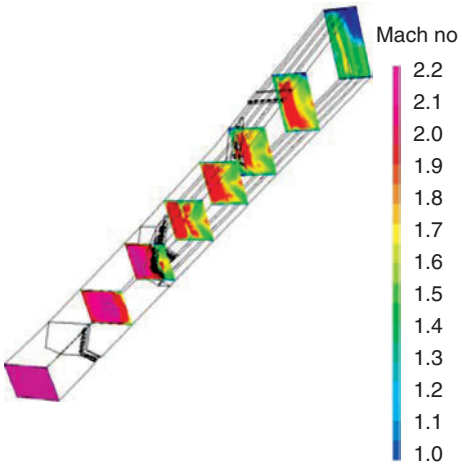

Figure 17. Mach number distribution at X/h = 0.0, 3.5, 5.8, 8.1, 10.5, 12.8, 16.3 and 21.5.

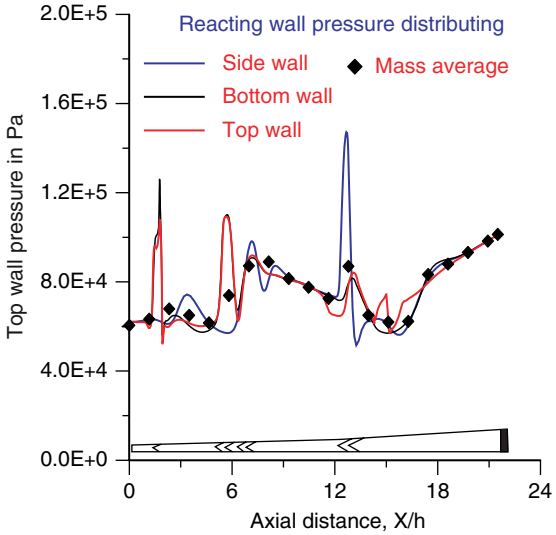

Figure 18. Comparison of axial distribution of surface pressure at top wall, bottom wall and side wall.

compared for the old and new strut designs in Fig. 19. We can observe that, for new strut arrangements, a significant amount of CO_2 has been produced in the near wall region and the zones of reaction are more spread and intensive. The axial distributions of combustion efficiencies between the two cases are presented in Fig. 20.

Following Kim et al. [34], combustion efficiency is defined as

$$\eta_c(x) = 1 - \frac{\int \rho u Y_F dA}{(\rho u Y_F dA)_{x=0}}$$

Where Y_F is the mass fraction of kerosene fuel.

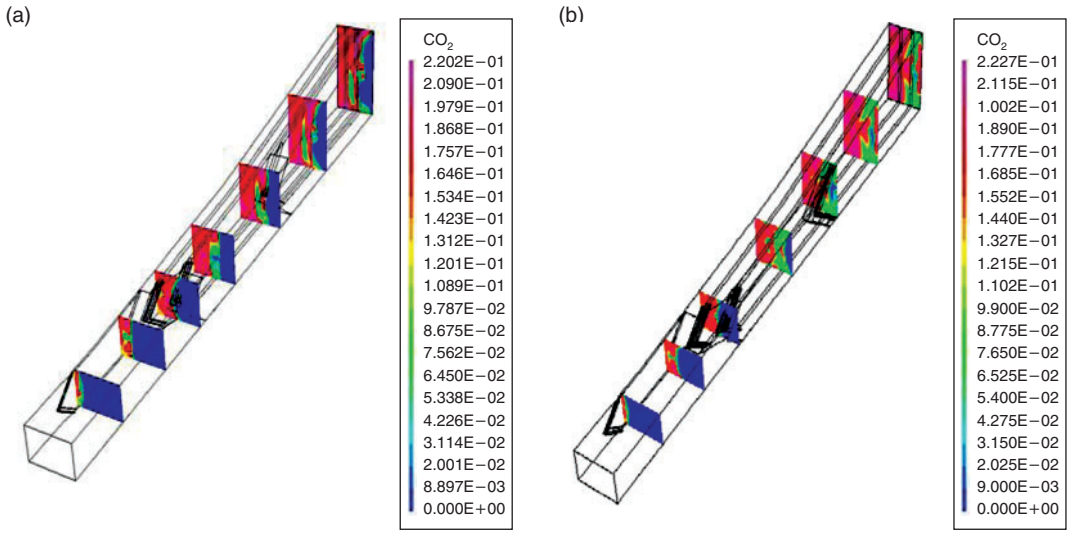

Figure 19. Comparison of axial distribution of CO_2 mass fraction distribution (a) old strut arrangement (b) New strut arrangement.

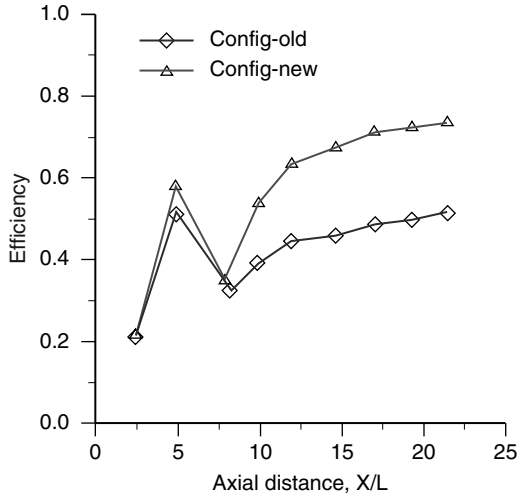

Figure 20. Axial distributions of combustion efficiencies between two strut arrangements.

A significant improvement in combustion efficiency for the new strut arrangement is observed and the computed combustion efficiency at the combustor exit is 73.4%.

The combustor so designed was tested [35] and the comparisons of the top wall surface pressure for the reacting case are presented in Fig 21. The simulation results for supersonic outflow boundary condition are also presented in the same figure to show the location of flow separation in the combustor. The computed pressure is lower than the experimental value in the mid-region of the combustor. The match in the divergent portion of the combustor is reasonable. The reason for the mismatch in the fuel injection zone is not clear. Because of the use of fast chemistry in the simulation, we expected the computed pressure would be higher than the experimental value. However, this mismatch in the near constant area cross section of the combustor will not alter the combustor performance significantly.

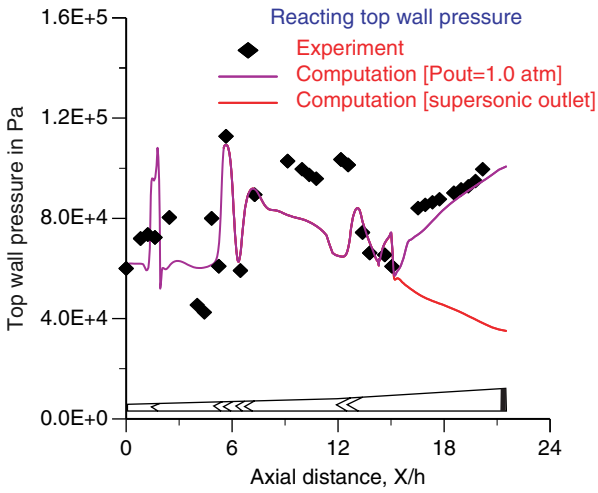

Figure 21. Comparison of experimental and computational surface pressure at top wall.

4. CONCLUSIONS

Numerical simulations were carried out for the design and analysis of strut based kerosene fueled scramjet combustor. The commercial CFD software CFX-TASCflow with K-ε turbulence model was used to solve three dimensional Navier Strokes Equations. Combustion was modeled using the Eddy Dissipation Concept based on infinitely fast kinetics. The evaporation and mixing of liquid kerosene droplet is studied by employing a Lagrangian Dispersed Phase Analysis. A detailed validation of the software has been carried out by comparing reliable experimental results of various reacting flow cases pertaining to scramjet combustor flow fields with both kerosene and hydrogen fuel with different fuel injection systems. It has been found that, although the predicted pressure rise is higher than the experimental value in the fuel injection zone because of fast chemistry assumption, the computed pressures match reasonably well in the divergent portion of the combustor where the major portion of thrust is produced. This validated numerical tool was then used for the design and analysis of a flight-sized scramjet combustor for an airbreathing mission. Computed flow parameters were analysed and design modification were carried out by relocating the struts and fuel injection system to achieve better performance of the combustor in terms of thrust and combustion efficiency. CFD tools are playing a very significant role in developing kerosene fuelled scramjet combustors for hypersonic airbreathing mission.

ACKNOWLEDGEMENTS

The work carried out by the scientists of the Computational Combustion Dynamics (CCD) Division of the Directorate of Computational Dynamics (DOCD), DRDL, Hyderabad are compiled and presented here. Author is thankful to all the members of CCD Division of DOCD for their help in preparing this paper. The author expresses his sincere thanks to Dr. V. Ramanujachari, scientist, DRDL for providing the experimental results for comparisons with CFD results.

REFERENCES

[1] A Ferri (1964): “Review of problems in application of Supersonic Combustion”, Journal of the Royal Aeronautical Society, Vol 68, No. 645, pp 575–597.

[2] E T Curran (2001): “Scramjet Engines: The first forty years”, Journal of Propulsion and Power, Vol 17, No.6, pp 1138–1148.

[3] Seiner, J.M., Dash, S.M. and Kenzakowski, D.C. (2001): “Historical survey on enhanced mixing in scramjet engines”, Journal of Propulsion and Power, Vol. 17, No. 6, pp 1273–1286.

[4] Masuya, G., Komuro, T., Murakami A., Shinozaki, N., Nakamura, A., Murayama, M. and Ohwaki, K. (1995): "Ignition and combustion performance of Scramjet combustor with fuel injection struts", Journal of Propulsion and Power, Vol 11, No. 2, pp 301–307.

[5] Mitani, T., Kanda T., Hiraiwa, T., Igarashi, Y. and Nakahashi, T. (1999): "Drags in Scramjet engine testing - Experimental and Computational Fluid Dynamics studies", Journal of Propulsion and Power, Vol 15(4), pp 578–583.

[6] Mitani T., Chinzei, N. and Kanda, T. (2001): "Reaction and Mixing-Controlled Combustion in scramjet engines", Journal of propulsion and power, Vol 17(2), pp 308–313.

[7] Gerlinger. P., Kasal, P., Stoll, P. and Bruggemann D. (2001): "Experimental and theoretical investigation on 2D and 3D parallel Hydrogen / air mixing in a supersonic flow", ISABE paper No 2001–1019.

[8] Tomioka, S., Murakami, A., Kudo, K. and Mitani, T. (2001): "Combustion tests of a staged supersonic combustor with a strut", Journal of Propulsion and Power, Vol 17(2), pp 293–300.

[9] Tomioka, S., Kobayashi, K., Kudo, K., Murakam, A. and Mitani, T. (2003): "Effects of injection configuration on performance of a stage supersonic combustor", Journal of Propulsion and Power, Vol 19, No. 5, pp 876–884.

[10] Glawe, D.D., Saminy, M., Nejad A.S. and Cheng, T.H. (1995): "Effects of nozzle geometry on parallel injection from base of an extended strut into a supersonic flow", AIAA paper 95–0522.

[11] Wepler U. and Kaschel W. (2002): "Numerical investigation of turbulent reacting flows in a scramjet combustor Model", AIAA paper No. 2002–3572.

[12] Mathur, T., Gruber, M., Jackson, K., Donbar, J., Donaldson, W., Jackson, T. and Billig, F. (2001): "Supersonic combustion experiments with a cavity-based fuel injector", Journal of Propulsion and Power, 17 (6), 1305–1312.

[13] Yu, G., Li, J.G., Chang, X.Y., Chen, L.H., and Sung, C.J. (2003): "Fuel Injection and Flame Stabilization in Liquid – Kerosene Fueled Supersonic Combustor," Journal of Propulsion and Power, Vol. 19 (5), pp. 885–893.

[14] Burnes, R., Parr, T.P., Wilson, K.J. and Yu, K. (2000): "Investigation of supersonic mixing control using cavities - Effects of fuel injection location", AIAA Paper 2000–3618.

[15] Yu, K H., Wilson, K.J. and Schadow, K.C. (2001): Effect of flame holding on supersonic – combustion performance", Journal of Propulsion and Power. Vol 17(6), pp 1287–1295.

[16] Hsu, K.Y., Carter, C., Crafton, J., Gruber, M., Donbar, J., Mathur, T., Schommer, D. and Terry, W. (2000): "Fuel distribution about a cavity flame-holder in supersonic flow", AIAA paper 2000–3585.

[17] Gruber, M.R., Donbar, J.M., Carter, C.D. and Hsu, K.Y. (2004): "Mixing and combustion studies using cavity-based flame holders in a supersonic flow". Journal of Propulsion and Power, Vol 20 (5), pp 769–778.

[18] Yu, G., Li, J.G., Chang, X.Y., Chen, L.H. and Sung, C.J. (2003): "Fuel injection and flame stabilization in liquid – kerosene fueled supersonic combustor". Journal of Propulsion and Power, Vol 19 (5), pp 885–893.

[19] Vinogradov, V. A., Kobigsky, S. A. and Petrov, M. D. (1995): "Experimental investigation of kerosene fuel combustion in supersonic flow", Journal of Propulsion and Power, Vol 11 (1), pp 130–134.

[20] Bouchez, M., Dufour, E., and Montazel, X. (1998): "Hydrocarbon fueled scramjet for hypersonic vehicles" AIAA paper 1998–1589.

[21] Dufour, E. and Bouchez, M. (2001): "Computational analysis of a kerosene fueled scramjet" AIAA paper 2001–1817.

[22] Manna, P. Behera, R. and Chakraborty, D. (2008): "Design and Analysis of Liquid Fueled Strut Based Scramjet Combustor – A CFD Approach", Journal of Propulsion and Power, Vol 24(2), pp 274–281.

[23] CFX-TASCflow Computational Fluid Dynamics Software, Version 2.11.1. AEA Technology Engineering Software Ltd. 2001.

[24] Saha, S. and Chakraborty, D. (2006): "Reacting flow computation of staged supersonic combustor with strut injection", AIAA Paper No. 2006–3895.

[25] Javed, A. and Chakraborty, D. (2006): "Numerical simulation of supersonic combustion of pylon injected hydrogen fuel in scramjet combustor" Journal of institute of engineers Vol 87, pp 1–6.

[26] Manna, P. Behera, R. and Chakraborty, D. (2007): "Thermochemical exploration of a cavity based supersonic combustor with liquid kerosene fuel" Journal of Aerospace Sciences and Technologies", Vol 59 (4), pp 246–258.

[27] Behera, R. and Chakraborty, D. (2006): "Numerical simulation of Kerosene Fueled Ramp Cavity Based Scramjet Combustor" Journal of Aerospace Sciences and Technologies, Vol 58 (2), pp 104–111.

[28] Kumaran, K. and Babu, V. (2009): "Investigation of the effect of chemistry models on the numerical prediction of supersonic combustion of hydrogen", Combustion and flame, Vol 156, pp 826–841.

[29] Gruenig, C., Avrashkov, V. and Mayinger, F. (2000): "Fuel injection into a supersonic airflow by means of pylons", Journal of Propulsion and Power, Vol 16 (1), pp 29–34.

[30] Gurenig, C., Avrashkov, V. and Mayinger, F. (2000): "Self-ignition and supersonic reaction of pylon injected hydrogen fuel", Journal of Propulsion and Power, Vol 16 (1), pp 35–41.

[31] Kumar, S., Charyulu, B. V. N., Moorthy, J. V. S. and Chandrasekhar, C. (2005), "Scramjet Combustor development", Newsletter, The Combustion Institute (Indian Section), Vol. 25, No. 4, April 2005, pp 16–31.

[32] Pannerselvam, S., Thiagarajan, V., Ganesh Anavardham, T.K., Geetha, J.J., Ramanuchari,V., and Prahlada (2005): "Airframe integrated scramjet design and performance analysis," ISABE Paper 2005–1280.

[33] "Supersonic combustion test in a 8000 fps air stream", Report No. 6064, June, 1964, Marquardth Corporation, Van Nuys, California, USA.

[34] Kim, J.H., Yoon, Y., Jenng, I. S., Hug. H. and Choi J.Y. (2003): "Numerical study of mixing enhancement by shock where in model scramjet engine", AIAA J, Vol 41 (6), pp 1074–1080.

[35] C. Chandrasekhar, D.K. Tripathi, V. Ramanujachari, S. Panneerselvam (2007): "Experimental investigation of strut based supersonic combustor burning hydrocarbon fuel", XVIII Annual ISABE Symposium, AIAA Paper No. 2007–1175.